THE EXCEPTIONAL IBERIAN HEATWAVE OF SUMMER 2018

D. Barriopedro, P. M. Sousa, R. M. Trigo, R. García-Herrera, and A. M. Ramos

August 2018 saw the warmest Iberian heatwave since that of 2003. Recent climate change has exacerbated this event making it at least »1°C warmer than similar events since 1950–83.

The summer of 2018 was exceptionally warm in Europe, with outstanding temperatures over widespread non-contiguous areas, including Scandinavia, central Europe, Iberia, and the British Isles (e.g., WMO 2019). Different from other extraordinary summers, extreme temperatures did not occur during the same weeks everywhere, hitting the British Isles in June, Scandinavia and central Europe in July, and southwestern Europe in August. Together, they yielded the warmest European summer of the last 519 years, above the record-breaking summers of 2003 and 2010, albeit by a small margin, as inferred from instrumental and proxy data (Fig. 1a). Although northern and central Europe captured the attention of the media, Spain and Portugal experienced the warmest August after that of 2003 (AEMET 2019; IPMA 2019). Temperature anomalies were more pronounced during daytime over southwestern Iberia, and Portugal saw its warmest month in maximum temperature (TX) since 1931. Heat peaked during 1–7 August 2018, when an exceptional heatwave caused four (two) out of the five warmest days of the twenty-first century in Portugal (Spain), with country-mean daily TX reaching 41.6°C (36.4°C). We use observational and reanalysis data for 1950–2018 to quantify recent changes in the intensity of this kind of events.

METHODS. We describe the exceptionality (Fig. 1) and changing risk (Fig. 2) of the 2018 Iberian heatwave by using daily TX from E-OBS at 0.25° × 0.25° for 1950–2018 (Cornes et al. 2018) and historical series from the European Climate Assessment and Dataset (ECA&D) (Klein Tank et al. 2002) and the Instituto Português do Mar e da Atmosfera (IPMA). The atmospheric circulation is described with daily geopotential height at 500 hPa (Z500) and 2.5° × 2.5° from the NCEP–NCAR reanalysis (Kalnay et al. 1996). We use the analog method, which infers the probability distribution of a target field from the atmospheric circulation during the event (Stott et al. 2016, and references therein). Flow analog days are defined from their root-mean-square differences (RMSD) with the actual Z500 anomaly field over 20°W–10°E, 32.5°–50°N. We reconstructed the Iberian (10°W–3.5°E, 36°–43.5°N) mean TX by randomly picking one of the 20 best analogs for each heatwave day (1–7 August). This process was repeated 5,000 times with circulation analogs of the present (1984–2017) and past (1950–83) subperiods separately, building flow-conditioned distributions of Iberian TX for two different "worlds." Their comparison provides the overall changes in heatwave intensity, including those due to non-anthropogenic factors [see Sánchez-Benítez et al. (2018) for details].

AFFILIATIONS: Barriopedro—Instituto de Geociencias, Consejo Superior de Investigaciones Científicas–Universidad Complutense de Madrid, Madrid, Spain; Sousa and Ramos—Instituto Dom Luiz, Faculdade de Ciências, Universidade de Lisboa, Lisbon, Portugal; Trigo—Instituto Dom Luiz, Faculdade de Ciências, Universidade de Lisboa, Lisbon, Portugal, and Departamento de Meteorologia, Instituto de Geociências, Universidade Federal do Rio de Janeiro, Rio de Janeiro, Brazil; García-Herrera—Departamento de Física de la Tierra y Astrofísica, Facultad de Ciencias Físicas, Universidad Complutense de Madrid, Madrid, Spain, and Instituto de Geociencias, Consejo Superior de Investigaciones Científicas-Universidad Complutense de Madrid, Madrid, Spain
CORRESPONDING AUTHOR: David Barriopedro, david.barriopedro@csic.es

DOI:10.1175/BAMS-D-19-0159.1

A supplement to this article is available online (10.1175/BAMS-D-19-0159.2)

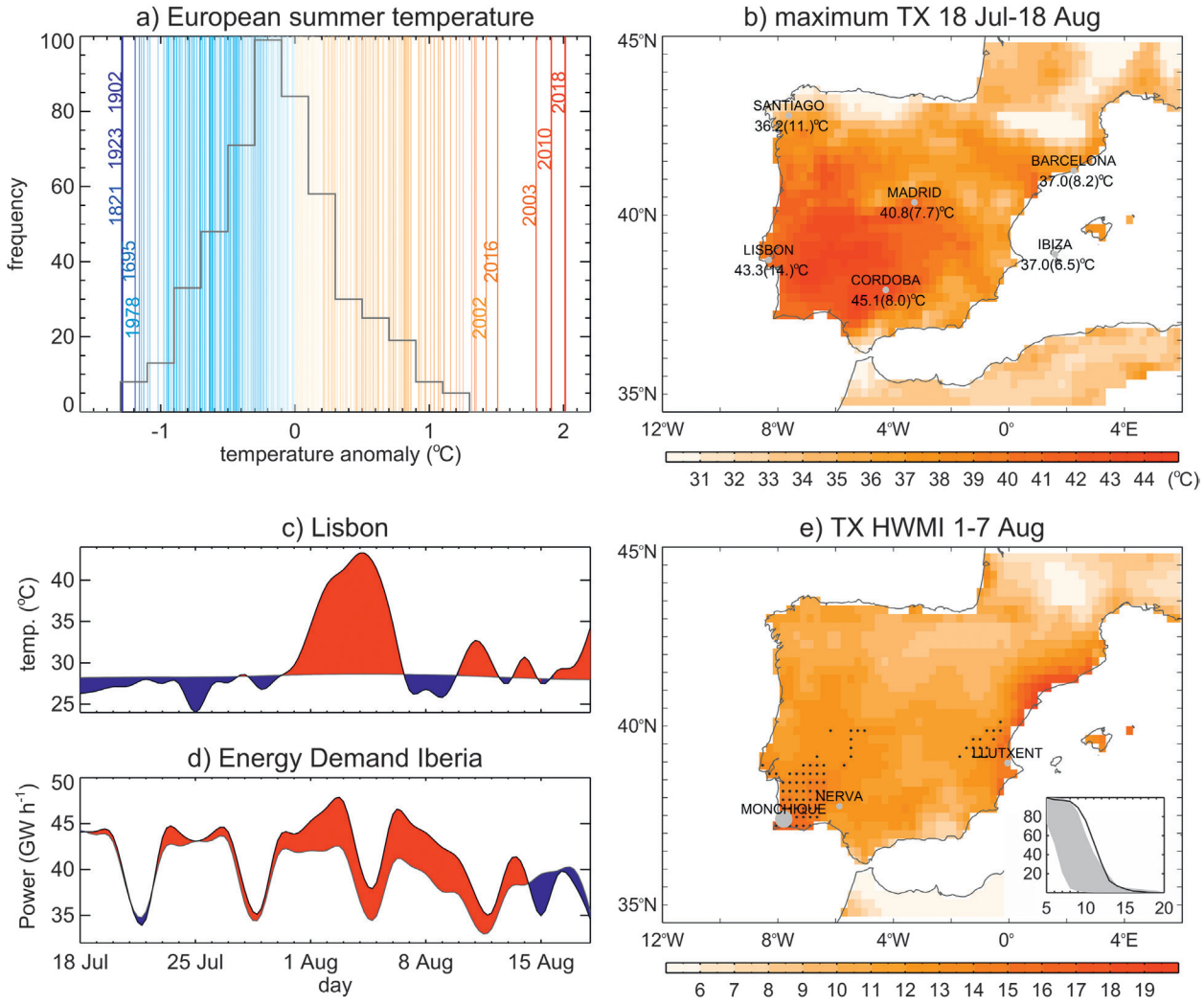

Fig. 1. (a) European summer land temperature anomaly (°C; wrt 1981–2010) over 25°W–40°E, 35°–70°N for 1500–2018 (lines) and its 1500–2000 frequency distribution (bars) using GISS (Hansen et al. 2010) for 1901–2018 and a multi-proxy reconstruction (Luterbacher et al. 2004). (b) Warmest daily TX for 18 Jul–18 Aug 2018 (shading) and selected stations (dots), with anomalies in parentheses (°C; wrt 1981–2010). Daily series of (c) Lisbon TX (°C) and (d) maximum electricity demand for Iberia (GW h^{-1}), with red (blue) denoting periods above (below) average (1981–2010 and week-equivalent days of 2013–17, respectively). (e) HWMI (dimensionless) for 1–7 Aug 2018 and percentage of Iberia exceeding a given value (inset plot, with the 1981–2000 5th–95th percentile range in shading). Black dots indicate record-breaking values (wrt all 7-day intervals of 18 Jul–18 Aug) and gray dots indicate major fires.

RESULTS. Figure 1b shows the highest TX of the 18 July–18 August 2018 period, which is close to the warmest 31-day interval of the year over Iberia. TX climbed to 46.8° and 46.6°C in weather stations of Portugal and Spain (both on 4 August), close to their national records. Although the highest TX occurred in southern and western Iberia (≫40% of the Portuguese stations broke their all-time records), unprecedented temperatures were also reported in central Iberia (e.g., 40.8°C, Madrid), the Mediterranean coast (e.g., 39.8°C, near Barcelona), and the Balearic Islands (e.g., 37.0°C, Ibiza). Likewise, minimum temperatures were exceptionally high, with more than 25% of the Portuguese stations setting absolute records and some Spanish locations reporting the warmest nights of the last century (e.g., 25.9°C, Madrid). Tropical nights affected 50% of Portugal and extended to the Mediterranean coast (e.g., >25°C, Barcelona) during seven consecutive days.

The first week of August saw the warmest anomalies (Fig. 2a, shading), as illustrated by the time series of Lisbon (Fig. 1c), where TX surpassed 40°C for three days, breaking its previous record twice by a large margin (≫2°C of exceedance). The atmospheric

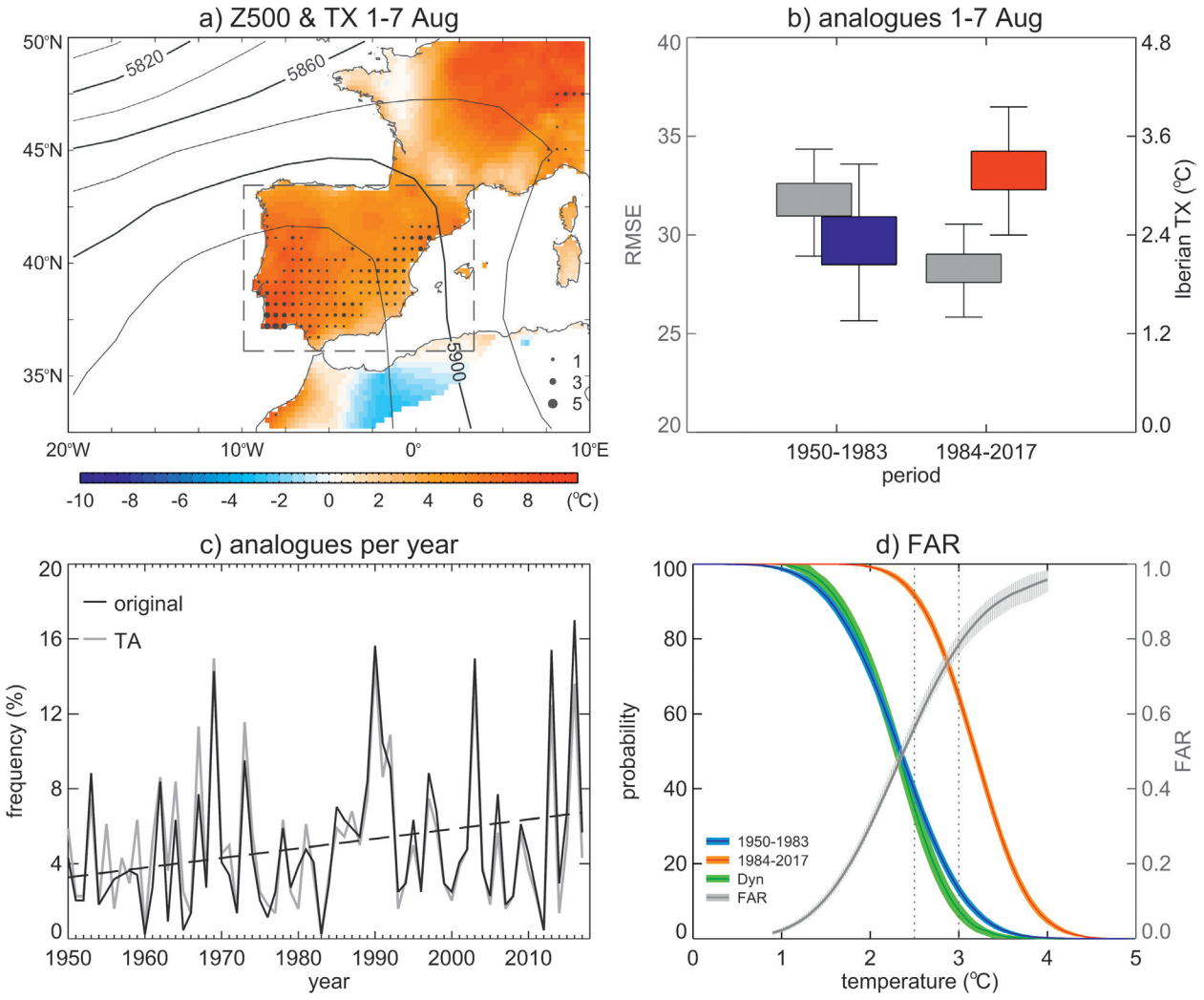

Fig. 2. (a) Z500 (m; contours) and TX anomaly (°C; shading) for 1–7 Aug 2018. Dots denote TX exceedance over previous records for that calendar period; (b) Flow-conditioned distributions of Iberian TX anomaly (°C; wrt 1981–2010; right *y* axis) for 1–7 Aug 2018 in past (1950–83; blue) and present (1984–2017; red) climates. Gray boxplots show their RMSD (left *y* axis); (c) Frequency series of good flow analogs (percentage of days) from raw (black) and detrended (gray) Z500 data. Dashed line indicates statistically significant trend ($p < 0.05$); (d) Past (blue) and present (red) flow-conditioned probabilities (%; left *y* axis) of Iberian TX anomaly above given thresholds (°C; *x* axis). The gray line represents the estimated FAR (dimensionless; right *y* axis) and the green line indicates the contribution of dynamical changes. Shading shows the 5th–95th percentile range from 1,000 random subsamples.

circulation displayed an outstanding subtropical ridge, with above-normal pressures extending to central Europe (Fig. 2a, contours). Enhanced stability and stagnant conditions worsened air quality, being aggravated by a Saharan dust episode (Sousa et al. 2019). Despite the wet and mild spring, two out of the three major Spanish fires of 2018 deflagrated during the heatwave, causing ≫4.500 ha of burned area and thousands of evacuated people. During 15 days (3–17 August), the largest European fire of 2018 devastated 27,000 ha in southern Portugal, surpassing the already unusual total area burned in Sweden (21,000 ha) or the United Kingdom (18,000 ha) all year round (San-Miguel-Ayanz et al. 2019). According to the media, daily mortality nearly doubled in Portugal (≫500 fatalities above the seasonal mean for 2–7 August) and some Spanish regions registered the highest number of deaths by heatstroke since official records started in 2004. Health-related impacts were partially minimized by an outsized use of air conditioning, which caused a 10% rise in Iberian energy consumption (Fig. 1d) and blackouts in Lisbon suburbs. Above-normal energy consumption extended beyond the heatwave, likely due to the concentration

of population in major touristic destinations, where the heat persisted the most. According to the Heatwave Magnitude Intensity (HWMI) index [Russo et al. 2015; also see the online supplemental material (SM)], more than half of Iberia experienced extreme HWMI values (unprecedented in the southern half of Portugal and some Mediterranean areas; Fig. 1e), resulting in the most intense Iberian heatwave on 7-day time scales since 1950 after the 2003 episode (Table ES1).

Figure 2b shows the distribution of Iberian TX averaged for the heatwave period, as inferred from flow analogs of the past (blue boxplot) and present (red) climate. Present-day analogs explain almost 60% of the observed Iberian TX, the remaining being attributed to non-dynamical processes (e.g., feedbacks) and limited sampling. The comparison reveals that similar atmospheric conditions trigger warmer Iberian TX ($\gg$1°C) now than in the recent past (i.e., the observed circulation would have caused a less severe heatwave in the past). This agrees with a warming and poleward trend of 2018-like Saharan intrusions, as reconstructed from flow analogs (see Fig. ES1 in the SM). Figure 2d quantifies how recent trends have changed the intensity of these Iberian heatwaves, by counting the fraction of replicated analogs with 7-day mean Iberian TX above a certain threshold in each subperiod. The flow-conditioned probability of experiencing Iberian heatwaves with TX anomalies above $\gg$2.5°C has doubled in just 35 years, equivalent to a fraction of attributable risk (FAR) of $\gg$0.5 (see the SM). Under the atmospheric circulation conditions of the 2018 heatwave, the chances of exceeding 3°C have risen by more than five times (FAR of 0.8).

CONCLUSIONS AND DISCUSSION. As the atmospheric circulation is constrained, the reported FAR should be attributed to thermodynamical changes (warming trend). However, flow analogs of the 2018 event show significant differences between the two subperiods, displaying smaller RMSD in the present than in the past (gray boxplots, Fig. 2b). Figure 2c (black line) confirms a significant ($p < 0.05$) upward trend in the 1950–2018 frequency series of "good" flow analogs, defined as those days with RMSD below the 5th percentile of the event distribution. This trend may reflect dynamical (e.g., Z500 gradients) changes or thermodynamical effects (e.g., thermal Z500 rise). To address this, we repeated the analysis by removing the regional monthly mean trends of Z500 and TX. The resulting thermodynamically adjusted (TA) distributions for the two subperiods become much closer and the trend in the number of good flow analogs is no longer significant at $p < 0.05$ (gray line, Fig. 2c). Their difference has been added to the past distribution to estimate the contribution of dynamical changes (green line, Fig. 2d). Dynamical changes cannot explain the changing risk of Iberian TX anomalies. Therefore, regional warming is largely responsible for the FAR, particularly in the higher TX thresholds. Further studies are encouraged to pin down the key drivers and their contributing roles to the reported changes (e.g., land–atmosphere feedbacks).

ACKNOWLEDGMENTS. We acknowledge the E-OBS dataset from http://www.uerra.eu (EU-FP6), the Copernicus Climate Change Service, the data providers in ECA&D (https://www.ecad.eu), IPMA, the GISTEMP Team 2019 dataset (data.giss.nasa.gov/gistemp/) and J. Luterbacher for providing the proxy-based reconstruction. Energy data were retrieved from https://demanda.ree.es/ and http://www.centrodeinformacao.ren.pt. AMR, PMS, and RMT were supported by project IMDROFLOOD (Improving Drought and Flood Early Warning, Forecasting and Mitigation using real-time hydroclimatic indicators; WaterJPI/0004/2014) through Fundação para a Ciência e a Tecnologia (FCT), Portugal. AMR was also supported by the Scientific Employment Stimulus 2017 from FCT (CEECIND/00027/2017). We thank three reviewers for their comments.

REFERENCES

AEMET, 2019: Resúmenes Climatológicos: Agosto de 2018. Agencia Estatal de Meteorología, accessed 5 January 2019, 11 pp., http://www.aemet.es/documentos/es/serviciosclimaticos/vigilancia_clima/resumenes_climat/mensuales/2018/res_mens_clim_2018_08.pdf.

Cornes, R., G. van der Schrier, E. J. M. van den Besselaar, and P. D. Jones, 2018: An ensemble version of the E-OBS temperature and precipitation datasets. *J. Geophys. Res. Atmos.*, **123**, 9391–9409, https://doi.org/10.1029/2017JD028200.

Hansen, J., R. Ruedy, M. Sato, and K. Lo, 2010: Global surface temperature change. *Rev. Geophys.*, **48**, RG4004, https://doi.org/10.1029/2010RG000345.

IPMA, 2019: Boletim Climatológico: Agosto 2018, Portugal continental. Instituto Português do Mar e da Atmosfera, accessed 5 January 2019, 16 pp., http://www.ipma.pt/resources.www/docs/im.publicacoes/edicoes.online/20180924/QyzZvZwgxxBnLFiHkSkX/cli_20180801_20180831_pcl_mm_co_pt.pdf.

Kalnay, E., and Coauthors, 1996: The NCEP/NCAR 40-Year Reanalysis Project. *Bull. Amer. Meteor.*

Soc., **77**, 437–471, https://doi.org/10.1175/1520-0477(1996)077<0437:TNYRP>2.0.CO;2.

Klein Tank, A. M. G., and Coauthors, 2002: Daily dataset of 20th-century surface air temperature and precipitation series for the European Climate Assessment. *Int. J. Climatol.*, **22**, 1441–1453, https://doi.org/10.1002/joc.773.

Luterbacher, J., D. Dietrich, E. Xoplaki, M. Grosjean, and H. Wanner, 2004: European seasonal and annual temperature variability, trends, and extremes since 1500. *Science*, **303**, 1499–1503, https://doi.org/10.1126/science.1093877.

Russo, S., J. Sillmann, and E. Fischer, 2015: Top ten European heatwaves since 1950 and their occurrence in the coming decades. *Environ. Res. Lett.*, **10**, 124003, https://doi.org/10.1088/1748-9326/10/12/124003.

Sánchez-Benítez, A., R. García-Herrera, D. Barriopedro, P. M. Sousa, and R. M. Trigo, 2018: June 2017: The earliest mega-heatwave of reanalysis period. *Geophys. Res. Lett.*, **45**, 1955–1962, https://doi.org/10.1002/2018GL077253.

San-Miguel-Ayanz, J., and Coauthors, 2019: Advance EFFIS Report on Forest Fires in Europe, Middle East and North Africa 2018. EUR 29722 EN, Joint Research Centre, 36 pp., https://doi.org/10.2760/262459.

Sousa, P. M., D. Barriopedro, A. M. Ramos, R. García-Herrera, F. Espírito-Santo, and R. M. Trigo, 2019: Saharan air intrusions as a relevant mechanism for Iberian heatwaves: The record breaking events of August 2018 and June 2019. *Wea. Climate Extremes*, **26**, 100224, https://doi.org/10.1016/j.wace.2019.100224.

Stott, P. A., and Coauthors, 2016: Attribution of extreme weather and climate-related events. *Wiley Interdiscip. Rev.: Climate Change*, **7**, 23–41, https://doi.org/10.1002/wcc.380.

WMO, 2019: WMO Statement on the State of the Global Climate in 2018. WMO-No. 1233, World Meteorological Organization, 39 pp., https://library.wmo.int/doc_num.php?explnum_id=5789.